

Arbitrary Control of Electromagnetic Flux in Inhomogeneous Anisotropic Media with Near-Zero Index

Jie Luo,¹ WeiXin Lu,¹ ZhiHong Hang,¹ HuanYang Chen,¹ Bo Hou,¹ Yun Lai,^{1,*} and C. T. Chan²

¹Department of Physics, Soochow University, 1 Shizi Street, Suzhou 215006, People's Republic of China

²Department of Physics, Hong Kong University of Science and Technology, Clear Water Bay, Kowloon, Hong Kong

(Received 29 July 2013; published 21 February 2014)

We propose a method to control electromagnetic flux in an almost arbitrary way in wavelength and subwavelength scales. The capability of subwavelength flux control is enabled by the evanescent waves induced in a class of inhomogeneous anisotropic media with a near-zero permittivity component. By designing the spatial profile of the other permittivity component in such inhomogeneous media, the flow and distribution of energy flux can be conveniently manipulated. This method provides another approach to efficiently control electromagnetic flux in nonmagnetic media.

DOI: 10.1103/PhysRevLett.112.073903

PACS numbers: 41.20.Jb, 42.25.Bs, 42.79.-e, 78.20.Ci

Recently, the advance in the fields of plasmonics [1–3] and metamaterials [4–13] has bestowed the ability of controlling electromagnetic flux in unprecedented ways. By utilizing the evanescent property of surface plasmons existing on metal surfaces, subwavelength controlling of electromagnetic waves has been achieved, leading to promising applications such as nanoscale plasmonic chips [1] and nanolasing [3]. Another significant advance in wave controlling techniques is the discovery of metamaterials, i.e., artificial materials designed to exhibit effective permittivity and permeability values not found in nature. Based on metamaterials, various unusual phenomena have been achieved such as negative refraction [7], superlensing [6,8], and hyperlensing [9]. In particular, the theory of transformation optics [10–13] has been proposed to utilize specially designed anisotropic inhomogeneous media to control electromagnetic waves in an arbitrary way, which makes amazing applications such as cloaking [10–13] possible.

Although controlling electromagnetic waves and flux are often assumed to be the same, there is actually a difference between them. From the formula of the Poynting vector $\mathbf{S} = \mathbf{E} \times \mathbf{H}$, we can see that electromagnetic flux \mathbf{S} can be controlled by manipulating either the electric field \mathbf{E} or magnetic field \mathbf{H} , instead of both fields. Based on this idea, we propose a method to control electromagnetic flux in an almost arbitrary way. In our approach, we can design the spatial profile of permittivity or permeability to control either the electric or magnetic fields, respectively. For transverse magnetic (TM) waves, nonmagnetic media is suitable. In contrast, transformation optics operates in a different manner as it requires designed spatial profiles for both permittivity and permeability and controls electric and magnetic fields simultaneously [10–13]. Our work also shows that subwavelength control of electromagnetic waves can be achieved without utilizing surface plasmons.

The system that we employ is a special kind of metamaterials known as zero-index metamaterials [14–41]. Subsets of such materials include epsilon-near-zero (ENZ) and mu-near-zero (MNZ) materials exhibiting near-zero permittivity and permeability, respectively. Some very unusual transmission properties have been discovered in such media, such as the squeezing and tunneling effects through a narrow junction area filled with ENZ materials between two waveguides [16–19]. However, up to now, most research has considered homogeneous and isotropic zero-index materials. In this work, we investigate *inhomogeneous* and anisotropic zero-index metamaterials with only one component of the permittivity tensor near zero. The other permittivity components can take arbitrary values that are larger than zero. Such anisotropy allows us to introduce inhomogeneity into the system. Specifically, we can design the spatial profile of the other permittivity component to be an arbitrary function of coordinates. It turns out that the electromagnetic flux can be conveniently controlled to route in an arbitrary way according to the spatial profile. This provides us a unique approach for flux manipulation.

Without loss of generality, we consider waves of TM polarization propagating in the x direction. The inhomogeneous media that we considered can thus be described by

$$\epsilon_x \rightarrow 0^+, \quad \epsilon_y = f(x, y) \gg \epsilon_x, \quad \mu = 1, \quad (1)$$

where ϵ_x and ϵ_y are the x and y components of the relative permittivity tensor, μ is the relative permeability, and $f(x, y)$ is the inhomogeneity profile of the inhomogeneous media. We note that the wavelength in the propagation direction has a normal value, i.e., $\lambda = \lambda_0 / \sqrt{\epsilon_y \mu} = \lambda_0 / \sqrt{f(x, y)} \ll \infty$, where λ_0 is the wavelength in free space. Here, we would like to emphasize that this system with $\epsilon_x \rightarrow 0^+$ is totally different from previously studied isotropic ENZ materials with $\epsilon_x = \epsilon_y \rightarrow 0^+$ or anisotropic

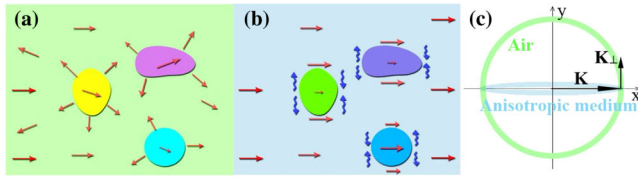


FIG. 1 (color online). Schematic illustration of wave propagation behaviors in (a) a normal inhomogeneous medium, and (b) an anisotropic inhomogeneous medium satisfying Eq. (1). (c) Equifrequency contours of the background media in (a) and (b).

ENZ metamaterials with $\epsilon_y \rightarrow 0^+$ [15–28], which both exhibit extremely long wavelengths in the propagation direction, i.e., $\lambda = \lambda_0 / \sqrt{\epsilon_y \mu} \rightarrow \infty$. As a result, the physics in our system is different from those in previous studies on zero-index metamaterials, and previous theories of ENZ materials based on $\lambda \rightarrow \infty$ [15–28] cannot be applied here.

If the inhomogeneity profile $f(x, y)$ is simply a constant in the whole space, then the value of ϵ_x does not have any influence on the wave propagation unless the propagation direction deviates from the x direction. However, if $f(x, y)$ is a spatially varying function, then the near zero ϵ_x would play a crucial role in the scattering mechanism.

In inhomogeneous media composed of ordinary materials, wave scatterings usually induce scattered propagating waves. In Fig. 1(a), we show the schematic picture of wave scattering by different scattering objects in air, where red arrows denote schematically the propagating and scattered waves. Since the scattered waves distribute energy flux in various directions, transmission in the forward direction is reduced.

However, in highly anisotropic media, the physics of scattering can be very different. In Fig. 1(b) we show the schematic picture of multiple scatterings in highly anisotropic media with $\epsilon_x \rightarrow 0^+$. Instead of producing propagating waves, the scatterings produce waves (shown as blue wavy arrows) that are evanescent in the forward and backward directions, and only capable of transferring energy flux in the perpendicular directions. The reason can be understood from the equifrequency contours of an isotropic medium of air (green) and a highly anisotropic medium of $\epsilon_x \rightarrow 0^+$ (blue), as shown in Fig. 1(c). Suppose that the scattering event is induced by a defect with a characteristic perpendicular length L_\perp , then a series of waves would be excited with perpendicular wave vectors K_\perp . For scattering events in air, when $L_\perp \geq \lambda$, K_\perp mostly fall within the maximum values of k_y of equifrequency contour (green circle). Excited waves are thus mostly propagating waves. While for scatterings in highly anisotropic medium of $\epsilon_x \rightarrow 0^+$, even when $L_\perp \geq \lambda$, K_\perp will fall outside of the maximum values of k_y of the equifrequency contour (blue flat ellipse). Evanescent waves are thus excited. Such a difference in the physical nature of scatterings leads to totally different transmission behaviors.

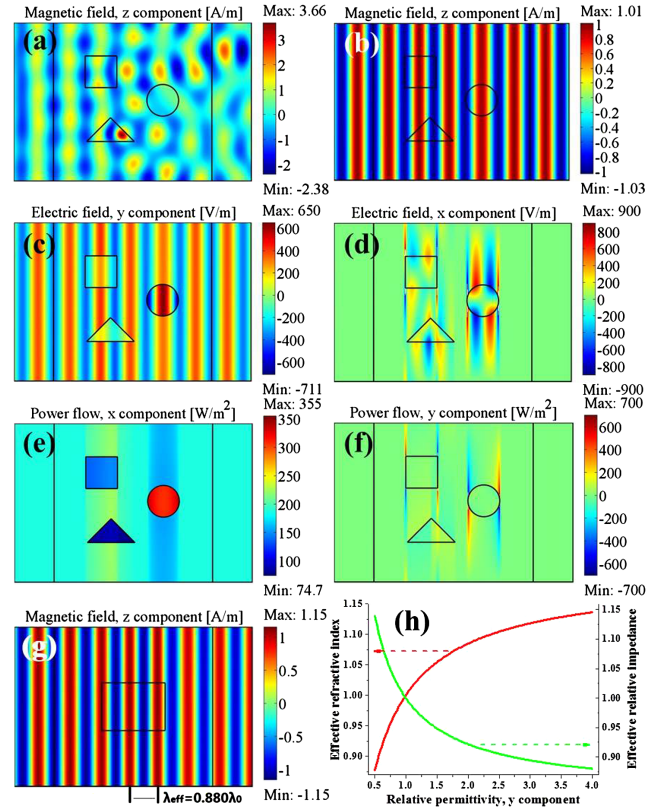


FIG. 2 (color online). (a) The field map of magnetic field H_z in a system of three isotropic defects with $\epsilon = 1.5$ (square), 2.5 (triangular), and 0.5 (circular) and $\mu = 1$ in an isotropic background, under an incident TM wave from the left. (b)–(f) show field maps of magnetic field H_z , electric field E_y , electric field E_x , energy flux S_x , and energy flux S_y , respectively, for the same system in (a) except for $\epsilon_x = 0.001$ throughout the whole system. (g) Field maps of magnetic field H_z in the system of a rectangular defect of $\epsilon_y = 4$ embedded in a background of $\epsilon_y = 1$, $\epsilon_x = 0.001$ and $\mu = 1$ throughout the whole system. (h) Dependence of effective refractive index and relative impedance on the ϵ_y value of the rectangular defect.

In the following, we demonstrate simulations of wave transmission by using the finite element software, COMSOL Multi-physics. First, we consider an inhomogeneous system composed of defects embedded in a background. For contrast, we first consider the case of three isotropic defects embedded in air. The defects have square, triangular, and circular shapes, and exhibit relative permeability $\mu = 1$ and permittivities $\epsilon = 1.5$, 2.5, and 0.5, respectively. Periodic boundary conditions are set on the upper and lower boundaries, and a TM-polarized plane wave is incident from the left, with a wavelength about the same size of the defects. From the magnetic field H_z , as shown in Fig. 2(a), we can see that strong scattered waves are excited, leading to distorted wave fronts and a reduced transmittance.

Next, we change the system to be highly anisotropic by letting $\epsilon_x = 0.001$, while keeping ϵ_y and μ unchanged in the

whole system. The wavelength $\lambda = \lambda_0 / \sqrt{\epsilon_y \mu} = \lambda_0$ and relative impedance $Z_r = \sqrt{\mu / \epsilon_y} = 1$ in the background is unchanged. In Figs. 2(b)–2(f), we show, respectively, the magnetic fields, electric fields in the y and x directions, and the power flow in the x and y directions under the same incident wave. The transmission behavior is dramatically altered. In Fig. 2(b), the magnetic field H_z is almost uniform in the y direction. Such uniformity is a result of the large anisotropy [42]. In Fig. 2(b), we also find that the transmittance is near unity, despite of the existence of three defects. We note that the shapes and materials of the defects have been chosen arbitrarily. This indicates that the high transmittance is not a resonance effect which would strongly depend on the details of inhomogeneity.

To understand the physical origin of such a robust high transmission, we look at the electric field in the y direction, i.e., E_y , in Fig. 2(c). It is seen that E_y is almost inversely proportional to ϵ_y , indicating that the displacement field $D_y = \epsilon_y E_y$ is almost uniform in the y direction. As a result, the time-averaged energy flux in the x direction, i.e., $\bar{S}_x = \frac{1}{2} \text{Re}(E_y H_z^*)$, is also inversely proportional to ϵ_y , as shown in Fig. 2(e). Since the total transmission is near unity, from the conservation law of energy flux, a proper amount of perpendicular flux, i.e., \bar{S}_y , must send flux to where \bar{S}_x is increased and from where \bar{S}_x is decreased. This is accomplished by evanescent waves. From Fig. 2(d), we find that evanescent waves are indeed induced within the x coordinate regimes with defects. In Fig. 2(f), we find that strong flux $\bar{S}_y = -\frac{1}{2} \text{Re}(E_x H_z^*)$ in the direction perpendicular to wave propagation emerges at the front and end positions of defects where the \bar{S}_x distribution changes. The evanescent-wave-induced \bar{S}_y is essential to keep the total flux $\int \bar{S}_x dy$ to be almost conserved throughout the whole media, leading to transmittance of almost unity.

Since the magnetic field H_z and electric displacement D_y are almost uniform in the y direction, effective medium theory in the quasistatic limit can be applied, and from which we obtain $\epsilon_{\text{eff}}(x) = h / \int (dy / \epsilon_y(x, y))$ and $\mu_{\text{eff}}(x) = \int \mu_z(x, y) dy / h$, where h is the height of the system. The effective refractive index and relative impedance are, respectively, $n_{\text{eff}} = \sqrt{\epsilon_{\text{eff}} \mu_{\text{eff}}}$ and $Z_{r, \text{eff}} = \sqrt{\mu_{\text{eff}} / \epsilon_{\text{eff}}}$. In Fig. 2(g), we show the case of rectangular defect of $\epsilon_x = 0.001$, $\epsilon_y = 4$, and $\mu = 1$ embedded in a background of $\epsilon_x = 0.001$, $\epsilon_y = 1$, and $\mu = 1$. Apparently, $\lambda_{\text{eff}} = \lambda_0 / n_{\text{eff}}$ is changed to be $0.880 \lambda_0$ due to the existence of the defect. In Fig. 2(h), we plot the obtained n_{eff} and $Z_{r, \text{eff}}$, which are obtained from the effective medium theory. Here, we can easily see that although the parameter change of the defect is relatively large, the impedance change is rather small, as a result of averaging in ϵ_{eff} and μ_{eff} . Thus, the robust high transmittance through the media is a result of the averaging effect due to the homogeneity of fields in the perpendicular direction of propagation.

The flux distribution $\bar{S}_x \propto 1 / \epsilon_y$ indicates that energy flux tends to concentrate where ϵ_y is small. By utilizing this

property, we can control how the electromagnetic flux flows through the whole system in an almost arbitrary way. In the following, we demonstrate three examples of electromagnetic flux control, including focusing of flux, splitting, and recombination of flux (cloaking in one dimension), and routing of flux in a sinusoidal path. Let $f(x, y)$ be smooth functions of inhomogeneity profiles within a square region of length a , as shown in Figs. 3(a), 3(c), and 3(e). In Figs. 3(b), 3(d), and 3(f), anisotropic gradient media of $\epsilon_y = f(x, y)$ and a constant $\epsilon_x = 0.001$ and $\mu = 1$ have been applied. The frequency is chosen to be $f = c / \lambda_0 = 5c / a$, where c is the velocity of light in free space. Perfect electric conductor (PEC) boundary conditions on upper and lower boundaries have been applied.

In the first example, we demonstrate the focusing of wave energy into a subwavelength area. The inhomogeneity profile $f(x, y)$ exhibits a minimum at the central area, as shown in Fig. 3(a). As a result, energy flux will be focused at the central point, as shown in Fig. 3(b). It is interesting to point out that the perpendicular size of the focused flux spot is about 0.27 times of the free space

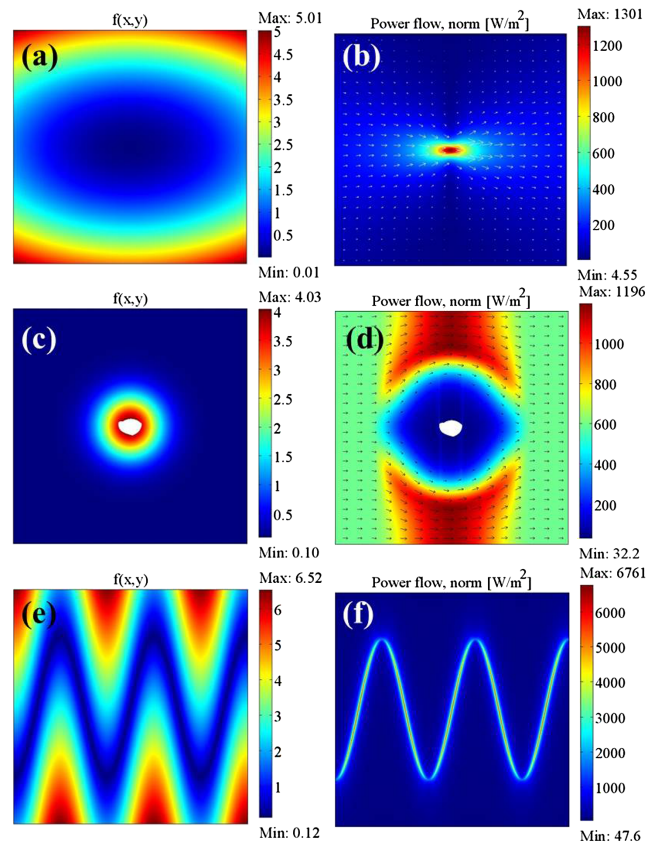


FIG. 3 (color online). The $\epsilon_y = f(x, y)$ distribution maps [(a), (c), and (e)] ($\epsilon_x = 0.001$ and $\mu = 1$ throughout the whole medium), total energy fluxes (color), and Poynting vectors (arrows) [(b), (d), and (f)] in three different gradient media, which demonstrate focusing of energy power [(a) and (b)], flux splitting [(c) and (d)], and free routing of energy flux in a designed sinusoidal path [(e) and (f)], respectively.

wavelength (see other fields in [42]). If we increase the wavelength, the focused flux spot would be even sharper. Therefore, subwavelength focusing can be realized with this method.

In the second example, we demonstrate the splitting and recombination of energy flux so as to realize “cloaking” in one dimension. As shown in Fig. 3(c), the inhomogeneity profile $f(x, y)$ exhibits a maximum at the central area where an irregular PEC shell is embedded. As a result, the energy flux is guided to go around the central area, rendering anything inside the PEC shell “cloaked,” as shown in Fig. 3(d). Although the phenomenon seems similar to invisibility cloaks in transformation optics, the physics behind is different, as we shall elaborate later.

In the third example, we have designed the inhomogeneity profile $f(x, y)$ to exhibit a sinusoidal pathway of minimal ϵ_y , as shown in Fig. 3(e). As a result, the energy flux indeed concentrates and flows along the designed sinusoidal path, as shown in Fig. 3(f). We note that the free space wavelength in Fig. 3(f) is about 10 times larger than the path width, which is about $0.02a$, indicating that this is a subwavelength control of flux. In this way, the energy flux can be conveniently controlled to flow along any desired curve in a sub-wavelength area.

One advantage of our approach here is that we can achieve flux control with nonmagnetic materials, as demonstrated in all of the above examples. This shows that the mechanism of controlling flux here is different from that of transformation optics. For transformation optics, the control of waves is achieved by reducing wave scattering to zero with designed gradient materials that are impedance matched everywhere and in every direction. While here, the control of flux is based on the excitation of evanescent waves, which efficiently transfers energy flux in the perpendicular direction of propagation. However, we should also note that unlike transformation optics, which does not depend on the form of incident waves, our approach only works for plane waves of normal incidence due to the zero permittivity index. Obliquely incident waves will be totally reflected at the surface of the system. In a word, such a flux controlling effect only works for a single mode.

In practical realization, unlike isotropic ENZ materials which are usually realized by Drude metal, semiconductors [20] or photonic crystals [21], anisotropic ENZ materials may be realized by using various kinds of metamaterials [19]. Interestingly, most of the previously designed metamaterials only involve resonance in one direction and are therefore automatically anisotropic. For one example, metal wire arrays [4,43] or metal-dielectric multilayers [44–46] may be used as anisotropic ENZ materials. If the system is composed of more than two materials, then it is possible to simultaneously achieve fixed near-zero and spatially varying nonzero permittivities in two orthogonal directions by tuning the material parameters and the filling fractions.

As another example, for transverse electric polarized waves, anisotropic MNZ materials with a near-zero permeability component are required instead of ENZ materials and split rings are just the perfect choice for anisotropic MNZ materials [5,37,41]. Actually, as a special manifestation of the flux control effect shown in this work, a bending waveguide based on anisotropic zero-index materials has been designed [40] and experimentally verified in the transverse electric polarization by using split rings [41] recently.

In practical metamaterial designs, loss is inevitable. We have examined the lossy cases in which ϵ_x not only has a near-zero real part but also carries an imaginary part. Interestingly, we find that loss does not compromise the flux controlling effect, but the major effect is to reduce the transmission rate. Even if the imaginary part of ϵ_x is 10 times larger than its real part, a strong ability to control the flux in the vertical direction of propagation is still preserved [42]. We also note that the issue of loss has been extensively discussed in the field of plasmonics and various schemes have been proposed to mitigate the problem [47]. Another way to avoid the loss problem is to use zero-index materials with less loss, e.g., dielectric materials [21], or to operate in the microwave regime [4,5] in which zero-index metamaterials have been experimentally verified to exhibit less loss and long transmission distances [19,37,41].

In summary, we have studied the behavior of electromagnetic wave propagation in a form of inhomogeneous ENZ materials with only one permittivity component near zero. We find scattered waves that are evanescent in the propagation direction lead to robust high transmittance, and also enable a unique way to arbitrarily control electromagnetic flux in wavelength and subwavelength scales. Our finding may inspire ideas leading to more functional and more compact devices.

This work is supported by the State Key Program for Basic Research of China (No. 2012CB921501), National Natural Science Foundation of China (No. 11104196, No. 11004147, No. 11104198, No. 11374215, No. 11374224), Natural Science Foundation of Jiangsu Province (No. BK2011277, No. BK20130281), Program for New Century Excellent Talents in University (NCET), and a Project Funded by the Priority Academic Program Development of Jiangsu Higher Education Institutions (PAPD). Work in Hong Kong is supported by Hong Kong RGC GRF Grant No. 600311.

*laiyun@suda.edu.cn

- [1] E. Ozbay, *Science* **311**, 189 (2006).
- [2] S. A. Maier, *Plasmonics: Fundamentals and Applications* (Springer, Berlin, 2007).
- [3] R. F. Oulton, V. J. Sorger, T. Zentgraf, R.-M. Ma, C. Gladden, L. Dai, G. Bartal, and X. Zhang, *Nature (London)* **461**, 629 (2009).

- [4] J. B. Pendry, A. J. Holden, W. J. Stewart, and I. Youngs, *Phys. Rev. Lett.* **76**, 4773 (1996).
- [5] J. B. Pendry, A. J. Holden, D. J. Robbins, and W. J. Stewart, *IEEE Trans. Microwave Theory Tech.* **47**, 2075 (1999).
- [6] J. B. Pendry, *Phys. Rev. Lett.* **85**, 3966 (2000).
- [7] R. A. Shelby, D. R. Smith, and S. Schultz, *Science* **292**, 77 (2001).
- [8] N. Fang, H. Lee, C. Sun, and X. Zhang, *Science* **308**, 534 (2005).
- [9] D. Lu and Z. Liu, *Nat. Commun.* **3**, 1205 (2012).
- [10] J. B. Pendry, D. Schurig, and D. R. Smith, *Science* **312**, 1780 (2006).
- [11] U. Leonhardt, *Science* **312**, 1777 (2006).
- [12] D. Schurig, J. J. Mock, B. J. Justice, S. A. Cummer, J. B. Pendry, A. F. Starr, and D. R. Smith, *Science* **314**, 977 (2006).
- [13] J. B. Pendry, A. Aubry, D. R. Smith, and S. A. Maier, *Science* **337**, 549 (2012).
- [14] S. Enoch, G. Tayeb, P. Sabouroux, N. Guerin, and P. Vincent, *Phys. Rev. Lett.* **89**, 213902 (2002).
- [15] R. W. Ziolkowski, *Phys. Rev. E* **70**, 046608 (2004).
- [16] M. Silveirinha and N. Engheta, *Phys. Rev. Lett.* **97**, 157403 (2006).
- [17] M. Silveirinha and N. Engheta, *Phys. Rev. B* **75**, 075119 (2007).
- [18] B. Edwards, A. Alù, M. E. Young, M. Silveirinha, and N. Engheta, *Phys. Rev. Lett.* **100**, 033903 (2008).
- [19] R. Liu, Q. Cheng, T. Hand, J. J. Mock, T. J. Cui, S. A. Cummer, and D. R. Smith, *Phys. Rev. Lett.* **100**, 023903 (2008).
- [20] D. C. Adams, S. Inampudi, T. Ribaudo, D. Slocum, S. Vangala, N. A. Kuhta, W. D. Goodhue, V. A. Podolskiy, and D. Wasserman, *Phys. Rev. Lett.* **107**, 133901 (2011).
- [21] X. Huang, Y. Lai, Z. H. Hang, H. Zheng, and C. T. Chan, *Nat. Mater.* **10**, 582 (2011).
- [22] J. Hao, W. Yan, and M. Qiu, *Appl. Phys. Lett.* **96**, 101109 (2010).
- [23] V. C. Nguyen, L. Chen, and K. Halterman, *Phys. Rev. Lett.* **105**, 233908 (2010).
- [24] Y. Jin and S. He, *Opt. Express* **18**, 16587 (2010).
- [25] Y. Xu and H. Chen, *Appl. Phys. Lett.* **98**, 113501 (2011).
- [26] J. Luo, P. Xu, L. Gao, Y. Lai, and H. Chen, *Plasmonics* **7**, 353 (2012).
- [27] Y. Wu and J. Li, *Appl. Phys. Lett.* **102**, 183105 (2013).
- [28] T. Wang, J. Luo, L. Gao, P. Xu, and Y. Lai, *J. Opt. Soc. Am. B* **30**, 1878 (2013).
- [29] B. Edwards and N. Engheta, *Phys. Rev. Lett.* **108**, 193902 (2012).
- [30] Y. Sun, B. Edwards, A. Alù, and N. Engheta, *Nat. Mater.* **11**, 208 (2012).
- [31] Mario G. Silveirinha and N. Engheta, *Phys. Rev. Lett.* **102**, 103902 (2009).
- [32] L. V. Alekseyev, E. E. Narimanov, T. Tumkur, H. Li, Y. A. Barnakov, and M. A. Noginov, *Appl. Phys. Lett.* **97**, 131107 (2010).
- [33] G. Subramania, A. J. Fischer, and T. S. Luk, *Appl. Phys. Lett.* **101**, 241107 (2012).
- [34] Ernst Jan R. Vesseur, T. Coenen, H. Caglayan, N. Engheta, and A. Polman, *Phys. Rev. Lett.* **110**, 013902 (2013).
- [35] S. Feng, *Phys. Rev. Lett.* **108**, 193904 (2012).
- [36] A. Alù, M. G. Silveirinha, A. Salandrino, and N. Engheta, *Phys. Rev. B* **75**, 155410 (2007).
- [37] Q. Cheng, W. X. Jiang, and T. J. Cui, *Phys. Rev. Lett.* **108**, 213903 (2012).
- [38] J. Luo, Y. Xu, H. Chen, B. Hou, W. Lu, and Y. Lai, *Europhys. Lett.* **101**, 44001 (2013).
- [39] A. A. Basharin, C. Mavidis, M. Kafesaki, E. N. Economou, and C. M. Soukoulis, *Phys. Rev. B* **87**, 155130 (2013).
- [40] J. Luo, P. Xu, H. Chen, B. Hou, L. Gao, and Y. Lai, *Appl. Phys. Lett.* **100**, 221903 (2012).
- [41] H. F. Ma, J. H. Shi, W. X. Jiang, and T. J. Cui, *Appl. Phys. Lett.* **101**, 253513 (2012).
- [42] See Supplemental Material at <http://link.aps.org/supplemental/10.1103/PhysRevLett.112.073903> for analytical expressions, a random example, comparison between different boundary conditions, details on field distribution, influences of anisotropy and loss, more examples, and description of simulation methods.
- [43] C. R. Simovski, P. A. Belov, A. V. Atrashchenko, and Y. S. Kivshar, *Adv. Mater.* **24**, 4229 (2012).
- [44] X. Ni, S. Ishii, M. D. Thoreson, V. M. Shalaev, S. Han, S. Lee, and A. V. Kildishev, *Opt. Express* **19**, 25242 (2011).
- [45] R. S. Savelev, I. V. Shadrivov, P. A. Belov, N. N. Rosanov, S. V. Fedorov, A. A. Sukhorukov, and Y. S. Kivshar, *Phys. Rev. B* **87**, 115139 (2013).
- [46] P. Ginzburg, A. V. Krasavin, A. N. Poddubny, P. A. Belov, Y. S. Kivshar, and A. V. Zayats, *Phys. Rev. Lett.* **111**, 036804 (2013).
- [47] S. Xiao, V. P. Drachev, A. V. Kildishev, X. Ni, U. K. Chettiar, H.-K. Yuan, and V. M. Shalaev, *Nature (London)* **466**, 735 (2010).